

WAKE: A Behind-the-ear Wearable System for Microsleep Detection

Nhat Pham^{†‡}, Tuan Dinh^{§‡}, Zohreh Raghebi^{††}, Taeho Kim[†], Nam Bui[†], Phuc Nguyen^{†*}, Hoang Truong[†], Farnoush Banaei-Kashani^{††}, Ann Halbower^{‡‡}, Thang Dinh^{§§} and Tam Vu^{†‡}

[†]University of Colorado Boulder, [‡]University of Oxford, [§]University of Wisconsin Madison,

^{††}University of Colorado Denver, ^{*}University of Texas at Arlington,

^{‡‡}Children's Hospital Colorado, ^{§§}Virginia Commonwealth University

{firstname.lastname}@colorado.edu, {firstname.lastname}@cs.ox.ac.uk, {firstname.lastname}@ucdenver.edu

tuan.dinh@wisc.edu, ann.halbower@childrenscolorado.org, tndinh@vcu.edu

ABSTRACT

Microsleep, caused by sleep deprivation, sleep apnea, and narcolepsy, costs the U.S.'s economy more than \$411 billion/year because of work performance reduction, injuries, and traffic accidents. Mitigating microsleep's consequences require an unobtrusive, reliable, and socially acceptable microsleep detection solution throughout the day, every day. Unfortunately, existing solutions do not meet these requirements.

In this paper, we propose a novel behind-the-ear wearable device for microsleep detection, called WAKE. WAKE detects microsleep by monitoring biosignals from the brain, eye movements, facial muscle contractions, and sweat gland activities from behind the user's ears. In particular, we introduce a Three-fold Cascaded Amplifying (3CA) technique to tame the motion artifacts and environmental noises for capturing high fidelity signals. The behind-the-ear form factor is motivated by the fact that bone-conductance headphones, which are worn around the ear, are becoming widely used. This technology trend gives us an opportunity to enable a wide range of cognitive monitoring and improvement applications by integrating more sensing and actuating functionality into the ear-phone, making it a smarter one.

Through our prototyping, we show that WAKE can suppress motion and environmental noise in real-time by 9.74-19.47 dB while walking, driving, or staying in different environments ensuring that the biosignals are captured reliably. We evaluated WAKE against gold-standard devices on 19 sleep-deprived and narcoleptic subjects. The Leave-One-Subject-Out Cross-Validation results show the feasibility of WAKE in microsleep detection on an unseen subject with average precision and recall of 76% and 85%, respectively.

CCS CONCEPTS

• **Computer systems organization** → **Embedded systems**; • **Human-centered computing** → **Mobile devices**; • **Hardware** → **Sensor devices and platforms**.

Permission to make digital or hard copies of all or part of this work for personal or classroom use is granted without fee provided that copies are not made or distributed for profit or commercial advantage and that copies bear this notice and the full citation on the first page. Copyrights for components of this work owned by others than ACM must be honored. Abstracting with credit is permitted. To copy otherwise, or republish, to post on servers or to redistribute to lists, requires prior specific permission and/or a fee. Request permissions from [permissions@acm.org](https://permissions.acm.org).

MobiSys '20, June 15–19, 2020, Toronto, ON, Canada

© 2020 Association for Computing Machinery.

ACM ISBN 978-1-4503-7954-0/20/06...\$15.00

<https://doi.org/10.1145/3386901.3389032>

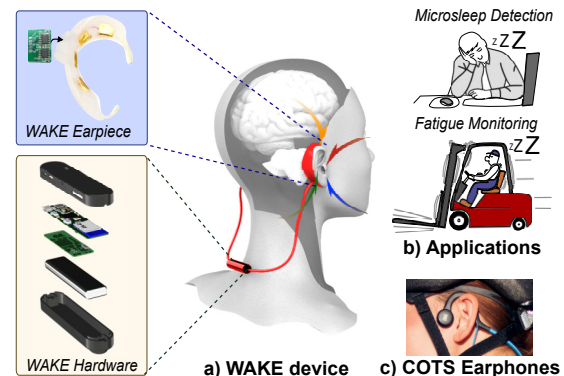


Figure 1: Biosignals monitoring from behind the ears concept.

KEYWORDS

Behind-the-ear sensing, Microsleep detection, Drowsiness monitoring, Fatigue supervising, Wearable devices, Cyber-Physical systems.

ACM Reference Format:

Nhat Pham, Tuan Dinh, Zohreh Raghebi, Taeho Kim, Nam Bui, Phuc Nguyen, Hoang Truong, Farnoush Banaei-Kashani, Ann Halbower, Thang Dinh and Tam Vu. 2020. WAKE: A Behind-the-ear Wearable System for Microsleep Detection. In *The 18th ACM International Conference on Mobile Systems, Applications, and Services (MobiSys'20)*, June 15–19, 2020, Toronto, Canada. ACM, New York, NY, USA, 15 pages. <https://doi.org/10.1145/3386901.3389032>

1 INTRODUCTION

More than half of the world's population suffers from sleep deprivation [63]. In the U.S, more than 65 million people suffer from Excessive Daytime Sleepiness (EDS) due to narcolepsy, obstructive sleep apnea, and sleep deprivation [76, 85]. EDS often results in frequent lapses in awareness of the environment (i.e. microsleeps). More than half of Narcoleptic people are unemployed [11, 21, 55, 111]. Moreover, Narcoleptic people often use Amphetamines to keep them awake, resulting in many drug overdose cases [7, 14, 33, 82]. Microsleep caused by sleep apnea alone leads to a loss of nearly \$150 million every year due to daily work performance reduction and vehicle accidents [81]. In addition, healthy people with sleep deprivation also experience microsleep [85]. Shift workers, night time security guards, and navy sailors with sleep problems have a 1.6x higher risk of being injured, causing 13% of all work injuries

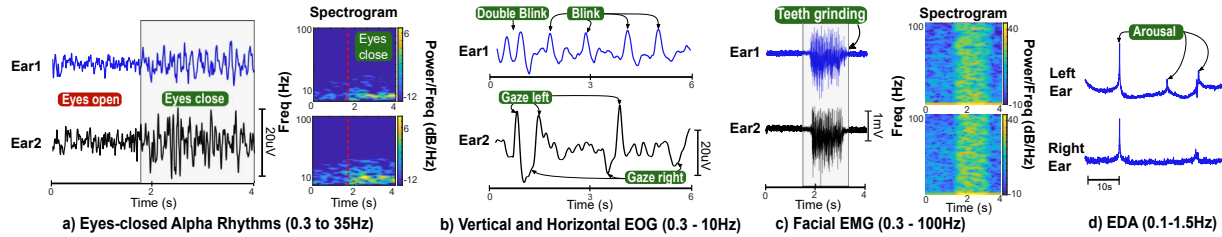


Figure 5: EEG, EOG, EMG and EDA signals captured from behind the ears.

the cerebrum, and the visual cortex. These neuronal activities are represented through brain waves, such as fast Beta (β) and Alpha (α) waves while the brain is wakeful and conscious, and the slow Theta (θ) waves when the brain experiences sleepiness. Furthermore, studies on animals [96, 109] have shown that Orexin neurons modulate pupil size, eyelid position, and possibly convergence and eye alignment via motoneurons of multiple muscle fibers. As a result, the wakefulness state is also represented by the movements and activities of the eyes. Additionally, several studies [26, 94] have shown that Orexin regulates wakefulness in the autonomic nervous system (ANS) by activating the ANS through projections to the ventrolateral medulla (VLM) and spinal cord causing the inhibition of sleep. The changes in sympathetic tone are, in turn, represented by changes in facial muscles and sweat gland activity.

Microsleep detection. Microsleep is the temporary episode of losing consciousness and is the key to capturing the transition from wakefulness to sleep [90, 95]. A microsleep episode can last from a few to 30 seconds and people can still wake up after an episode. Microsleep manifests itself both behaviorally (slow-rolling eyes, gradual eye-lid closure, head nods [46, 87]) and electrically (shift in electroencephalography (EEG) from fast α and β waves to slower θ activities [86, 90]). These manifestations link to the inhibition of the Orexin system [90]. Microsleep is extremely dangerous for tasks requiring constant awareness since people who experience MS are usually unaware of them and still believe that they are awake the whole time [45]. This often happens with people who have EDS.

Conventionally, the need for placing multiple sensors on the user's head to capture different biomarkers for accurate microsleep detection makes it challenging to build a wearable and socially acceptable system. As illustrated in Fig. 3b, several electrodes (e.g. at least 9 in the standard PSG system[13]) are usually needed to be placed on the user's scalp to capture brain waves. A wearable camera or 2-4 biopotential electrodes can be placed on the user's eyes to capture eye movements. To capture facial muscle contractions, electrodes are placed on the user's chin. Lastly, sweat gland activity is often captured by electrodes on the wrist or the fingers. With this amount of sensors at different locations on the user's head and face, achieving wearability and social acceptability for microsleep detection is not a trivial task. These studies confirm that there are four key bio-markers that we need to capture for microsleep detection. The remaining questions are (1) *where to place the sensors*, (2) *how many sensors are sufficient*, and (3) *how the sensors can be made to capture this information?* (Section. 3).

Impact of environmental noises and motion artifacts. Various noises and artifacts affect a wearable biosignal sensing system. Motion artifacts and electromagnetic interference from the environment are two major roadblocks for the practicality of the system.

Several approaches have been proposed to address the issues of artifacts and noise such as blind source separation with independent component analysis (ICA) [41, 114] or incorporating additional sensors such as inertial measurement units [19, 83]. These approaches, however, depend on a large number of electrodes to provide spatial information, require significant computation, and are difficult to implement in a real-time system [79]. Throughout our in-lab experiments using a PSG device, we found that environmental noises generate significant impacts on the original signal while human motion artifacts completely distort the whole signal, making it not even usable. *This requires a novel solution to remove these noises from the signals captured from wearable devices.* (Section. 5, 6)

3 EXPLORING MICROSLEEP BIOMARKERS FROM BEHIND THE EARS

As mentioned in the previous Section, the ear is the intersection of multiple microsleep biomarker sources (e.g. the brain, the eyes, facial muscles, and sweat glands) and is also a natural harbor point where a wearable device could be worn. While recent works [9, 37, 78, 120] on ear-based biosensing have shown the feasibility of capturing biosignals from the area behind the ears, monitoring microsleep-related biosignals have not been done before. Thus, it is unclear about (1) *where are the best places for EEG, EOG, EMG and EDA sensors to achieve wearability and sensing sensitivity*, (2) *what is the minimum number of required electrodes*, and (3) *what are the unique characteristics of BTE signals?*

The BTE electrodes placements. From our study on the ear anatomy, we derive the best sensor placement locations for microsleep detection, as shown in Fig. 3a and Fig. 4. At these locations, we can capture signals coming from the mid-brain area (EEG), eye movements (EOG), facial muscle contractions (EMG), and sweat gland activities (EDA). These sensor locations allow us to design a socially-acceptable wearable device that is well-hidden behind the user's ears just like commercial off-the-shelf (COTS) earphones.

Fig. 4 illustrates the anatomy of the temporal bone covering the whole BTE area. It consists of two major parts, i.e. the Squamous and Mastoid processes[32]. To capture EEG generated by the mid-brain area, we would want to place the electrodes on the Squamous process, which is the thin upper part of the temporal bone. This makes electrodes as close to the brain as possible. Two electrodes, i.e. channel 1 on the left ear and channel 2 on the right ear, are used to capture EEG on both sides of the brain. To capture EOG, i.e. vertical EOG (vEOG) and horizontal EOG (hEOG), we need to maximize the vertical and horizontal distance between each pair of electrodes, respectively. Thus, we place the reference electrode on the Mastoid process, which is the thick lower part. With this setup, channel 1 can pick up eye blinks and up/down movements, while

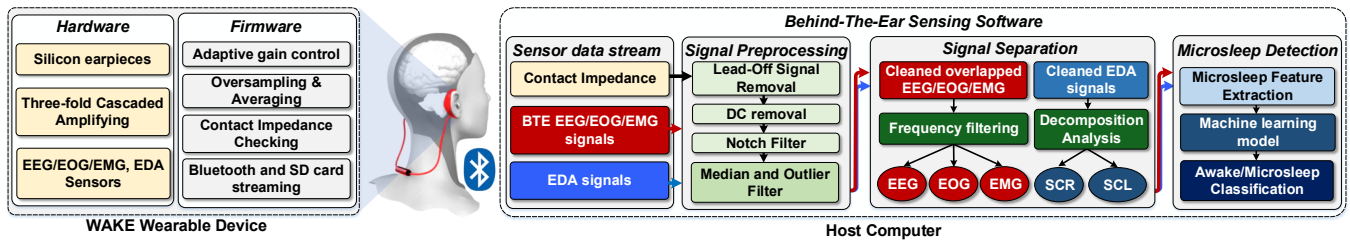


Figure 6: WAKE system overview.

channel 2 can capture the eyes' left and right movements. Additionally, both channel 1 and 2 can capture most of the facial muscle activities that link to the muscle group beneath the area behind the ears. Since EEG, EOG, and EMG are biopotential signals, we can use the same electrodes. Thus, we only need four electrodes, including two signal electrodes, a reference, and a common ground, to capture them. Capturing EDA behind the ear is promising because it has high sweat gland density [103]. As sweat gland activities are not symmetric between two halves of the body [88], placing two electrodes on each ear is necessary to reliably capture EDA.

Examining BTE signals. Signals captured from BTE electrodes resemble the most important biomarkers of microsleep that we would expect from standard electrodes placements (i.e., EEG, EOG, EMG, and EDA), as shown in Fig. 5. In particular, Fig. 5a presents the α rhythms seen on both BTE leads when the eyes are closed. Similarly, the same features, such as eye blinks, left gaze, right gaze, teeth grinding, and emotional arousal can be captured with BTE electrodes, as shown in Fig. 5b, c, and d, respectively. Thus, the results confirm that we could capture the aforementioned microsleep features from only behind the ears.

There are unique challenges to BTE signals. First, BTE signals are much smaller than the ones expected with standard placements. Particularly, the amplitude of EEG and EOG captured from BTE are all less than 50 μ V, which are much smaller than standard placements (100-500 μ V)[36]. This is probably because BTE electrodes are far from the signal sources of EEG and EOG. Secondly, we notice a significant amplitude difference (i.e. three orders of magnitude) between BTE EEG/EOG and EMG signals, as BTE EMG events could be as strong as a few millivolts. Moreover, the spectrogram in Fig. 5 shows that BTE EMG events have very strong power in all frequency bands from 0.3 to 100Hz. As we use the same BTE electrode to capture EEG, EOG, and EMG, addressing the overlap among these three signals is not trivial with filtering. Low BTE EEG/EOG signal amplitudes, combine with the fact that they overlap with EMG with significant amplitude difference at each BTE electrode, making it challenging to ensure high fidelity microsleep features while being robust against environmental noise and motion artifacts.

4 SYSTEM OVERVIEW

We design WAKE to include four main components (Fig. 6): (1) a motion mitigation sensing hardware using the 3-folds Cascaded Amplifying (3CA) technique, (2) a firmware adaptively amplifies of the signals; (3) a software running on a host device to process data from BTE sensors and detect user's microsleep; and (4) an ear-worn device designed for long-time usage.

WAKE hardware. We design a highly sensitive sensing circuit (Fig. 7) to capture the brain waves (EEG), polarization signal created

by eyeball activities (EOG), facial muscle contractions (EMG), and electrodermal activities (EDA). In WAKE, we derive an approach called 3CA, allowing the system to minimize the impact of motion artifacts and environmental noises in real-time at hardware and firmware levels. The key idea is to utilize multiple buffering and amplifying stages with precision buffers and instrumentation amplifiers to address the effects of electrode fluctuation, cable shaking, and environmental interference (Sec. 5).

WAKE firmware. WAKE firmware is designed to control our sensing hardware so that data from four main sensors: EEG, EOG, EMG, and EDA can be captured reliably (Sec. 6). The key challenges are that the signals are often weak and overlap each other. Thus, we design the firmware with three main components (1) adaptive gain control (AGC), (2) oversampling and averaging (OAA), and (3) Bluetooth and SD card streaming. AGC addresses the overlapping issue by dynamically changing the amplifier gain based on different signal types. Then, the OAA oversamples locally and averages data before streaming to the host device to ensure high signal to noise ratio while cutting down the power consumption of communication. The collected data is streamed over Bluetooth and to an SD card for later analysis.

WAKE algorithms. WAKE algorithms are implemented on a host device (i.e., mobile phones, laptops, etc.). Upon receiving the signals from the WAKE ear-worn device, the data are separated into different streams and ready for further processing. There are three main data streams are collected including a BTE EEG/EOG/EMG signals, EDA signal, and contact impedance signal. During signal pre-processing, the DC, electricity noises, and other noises are removed by DC removal, notch, median, and outlier filters, respectively. The clean EEG, EOG, EMG, and EDA signals obtained from pre-processing are then used for microsleep classification. The features extracted from these signals are later used to together with a set of machine learning algorithms to detect microsleep.

WAKE earpieces. WAKE system is designed for comfortable, reliable, cost-effective, and continuously collecting behind the ear signals. To realizing that goal, we design the earpieces by carefully sketching the device architecture and then implementing them using off-the-shelf components. The earpieces materials were also carefully selected ensuring good contacts between the electrodes and the human skin as well as allowing it to be comfortably worn by users. We also validated and identified the most proper electrode materials that provide the highest sensitivity (Sec. 8).

In the next section, we will discuss our proposed solution to address one of the most important challenges of designing a reliable wearable device: "how to cancel the noises created by human motion artifacts and coupled from the environment?"

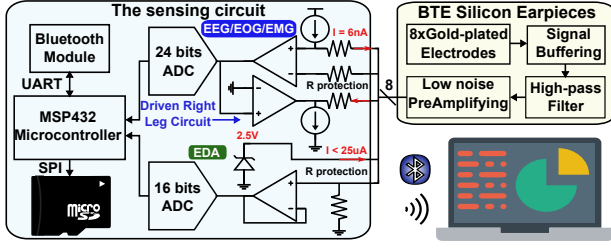


Figure 7: WAKE hardware module.

5 MITIGATING IMPACT OF MOTIONS & NOISE – A HARDWARE SOLUTION

Noises created by motion and coupled from the environment are important challenges that we need to overcome to ensure the reliability and practicality of WAKE. These noise span across all frequency of interest and are highly unpredictable, making their removal non-trivial from the signal by software methods such as filtering or ICA [24]. In literature, Active Electrodes (AE) [16, 122, 123] have been proposed to mitigate motion artifacts and environmental interference. However, conventional AE does not consider the unique characteristic of BTE signals, which are (1) weak EEG and EOG signal amplitudes, (2) signals overlap with three orders of magnitudes difference, and (3) limited spaces for BTE electrodes. We propose a technique called Three-fold Cascaded Amplifying (3CA) on the electrical pathway of WAKE. Fig. 8 presented the model for the 3CA technique with three stages: (1) Stage 1 – Unity Gain Amplifying, (2) Stage 2 – Feed Forward Differential PreAmplifying (F2DP), and (3) Stage 3 – Adaptive Amplifying. The first and second stages are implemented on our BTE earpieces, while the third stage is implemented on the sensing circuit and its firmware.

Stage 1 – Unity-gain amplifying. The root cause of motion artifacts lies in the fluctuations of the wires and micro-movements of electrodes [108]. These fluctuations create changes in the electrical pathway resulting in measurement noise. We address the motion artifacts by introducing the first stage: unity-gain amplifying (a.k.a buffering). Considering the reference circuit model, as in Fig. 8, V_s is the signal source from the ears, C_w is inherent capacitance on signal cables, and Z_c is the skin-electrode contact impedance. V_o , A , Z_i , R_i , C_i , Z_o , C_p are output voltage; ideal voltage gain; input impedance, resistance, and capacitance; output impedance; and parasitic capacitance of each amplifier.

Since the biosignals are extremely weak (i.e., μV level), instrumentation amplifiers are usually used to amplify the signals, making them available for further processing. When an instrumentation amplifier is used, we can model the effect of motion artifacts by using the voltage gain rule ($V_o = A * V_i$) and Kirchhoff's current and voltage laws (1) at the input of the amplifier:

$$(V_s - V_i)/(Z_{c1} + Z_{c2}) - (V_i)/(Z_i) + j\omega C_p(V_o - V_i) = 0. \quad (1)$$

By eliminating V_i from Eq. 1, we have a relationship among the actual gain ($G = V_o/V_s$) of the circuit, skin-electrode contact impedance (Z_{c1} , Z_{c2}), and the inherent capacitance on signal wires (C_w):

$$G = \frac{A}{1 + (Z_{c1} + Z_{c2})\left(\frac{1}{R_i} + j\omega(C_w + C_i - (A-1)C_p)\right)}. \quad (2)$$

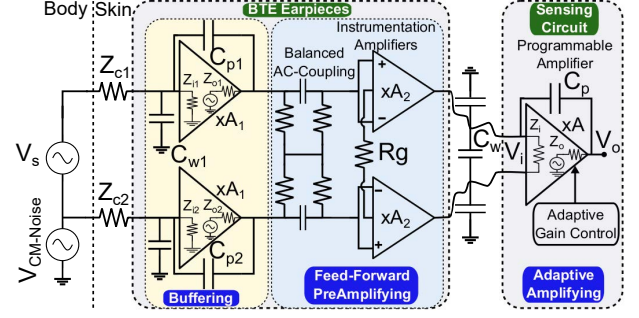


Figure 8: 3CA model.

As motions happen, cable sway and electrode movement create the fluctuation on C_w and $Z_{c1} + Z_{c2}$, respectively. This results in the fluctuation of the actual gain (G). To minimize the fluctuation effect of C_w (generated by triboelectric processes and change of parasitic capacitance in the measurement network [2, 100, 119]), we can use an op-amp buffer for each electrode to convert the high impedance lines (Z_{c1} , Z_{c2}) to approximately zero (Z_{o1} , $Z_{o2} \approx 0$). Rewrite Eq. 2 for the op-amp buffer in the first stage, we have

$$G = \frac{A_1}{1 + Z_{c1}\left(\frac{1}{R_{i1}} + j\omega(C_{w1} + C_{i1} - (A_1 - 1)C_{p1})\right)} = \frac{A_1}{1 + Z_{c1}\gamma}. \quad (3)$$

Ideally, the effect of Z_{c1} fluctuation can be removed if we can satisfy the following equation: $\gamma = 0$. While it is very challenging to achieve in practice, we still can make γ as close to 0 as possible. This could be done by using an ultra-high input impedance buffer, where $A_1 = 1$, $R_{i1} \rightarrow \infty$, and $C_{i1} \rightarrow 0$ in our first stage. Putting a buffer circuit directly on the electrodes is the best way to minimize C_{w1} . However, this is not desirable, as we have limited space for our BTE electrodes. We notice that as long as we keep C_{w1} small and stable, putting the circuit directly on the electrode is not needed. This is done by fixing the connection between each electrode and its buffer in a stable structure to avoid triboelectric noise and shielding it by using a micro-coax shielded cable. By driving the shield with the same voltage as the signal from the output of the amplifier, we effectively minimize C_{w1} . Up to this point, the unity-gain amplifying stage can remove the impact of human motion artifacts. The signals, however, need to go through another stage to remove all the environmental noise, as described in the following discussion.

Stage 2 – Feed Forward Differential PreAmplifying (F2DP). To ensure robustness against environmental interference, intuitively, we would want to preamplify our weak and overlapped BTE signals before driving the cables to our sensing circuit. Conventionally, if an amplifier with positive gain (>1) is used, the equation $\gamma = 0$ cannot be satisfied, making the system prone to motion artifacts. Furthermore, electrode contact impedance mismatch, which is often seen in practice, leads to the a gain mismatch among electrodes, as shown in Eq. 3. Gain mismatches between two electrodes will allow more common-mode noise to be coupled into the system. By dividing into unity-gain and F2DP stages with positive gain, we can overcome this challenge because the input impedance of F2DP is effectively close to 0. Thus, the effect of contact impedance will not affect the gain in the next stages.

Inspired by the robustness against noises of balanced audio systems where preamplified differential signals are generated before

transiting over wires, differential signaling is employed in our design. We apply the Feed-Forward (FF) differential amplifying technique, which has been shown by simulation in [54] to significantly increase the Common-Mode Rejection Ratio (CMRR), i.e. the ability to reject noise coupled from the environment, than using the conventional Driven Right-Leg circuit (DRL) by 49 dB. The FF topology used in [54], however, is not practical because its stability suffers from gains mismatch when two different gain resistors are used in the proposed topology. Mismatch in these resistors causes the output common-mode level to move with the output signal, resulting in distortion[57]. Thus, we employ the cross-connection technique where only one gain resistor (i.e., R_g in Fig. 8) is needed to set the gain for two FF instrumentation amplifiers in our F2DP. After F2DP, fully differential and preamplified signals are produced making them robust against environmental interference while driving the cables to the sensing circuit.

F2DP only works when the DC component is removed completely. We found that the traditional high pass RC filter approach is not efficient in removing the DC component (100x larger than signals of interest) because it introduces an additional ground-path and component mismatch, which reduces the efficiency of rejecting environmental noise of F2DP. Balanced AC-coupling topology [47] is a best-fit solution to overcome these challenges because it does not introduce any additional ground-path and minimizes the component mismatch since the pole and zero of the filter cancel themselves out. In particular, considering 'Balanced AC-coupling' components in Fig. 8, this topology does not include the ground-path, thereby eliminating its side-effects. Moreover, RC components are never precise in practice (approximately from 1% to 20% error for a capacitor) and their mismatch problem is difficult to solve. The chosen balanced AC-coupling topology dampens these mismatches by canceling the redundant poles and zeros created by component mismatch [47].

Stage 3 – Adaptive Amplifying. After the previous stage, the system can reliably collect BTE signals; we are now solving the problem of our BTE signals themselves. The unique challenge that we need to address with our BTE signals is the significant amplitude range differences between EEG/EOG and EMG signals (i.e. from μV level to mV level for EEG/EOG and EMG signals, respectively). This challenge has not been considered in the traditional EEG system, as EEG electrodes are placed far away from EMG sources. The difference leads to signal saturation at the ADC on the sensing circuit when EMG signals are amplified with the same gain as EEG/EOG signals. The CMRR of the amplifier is presented by the following equation: $CMRR = 10 * \log \frac{A_d^2}{A_{cm}^2}$, where A_d and A_{cm} are the differential and common-mode gain, respectively. In an instrumentation amplifier, A_{cm} is a constant depending on the internal resistors. Thus, CMRR only depends on A_d . Since the difference between EMG and EEG/EOG could be as large as three orders of magnitude, setting the gain too low to avoid EMG saturation will also significantly lower CMRR (up to 60 dB), increasing the noise floor to a level where EEG/EOG signal cannot be captured. We found that the gain needs to be dynamically adjusted in real-time so that both small EEG/EOG and large EMG signals are captured with high resolution. The key idea is to design a method that can identify the signal patterns and select the proper amplification gain (Sec. 6).

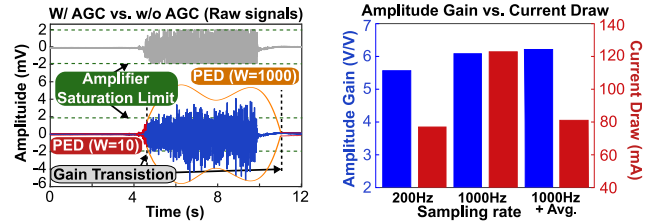


Figure 9: EMG saturation without AGC.

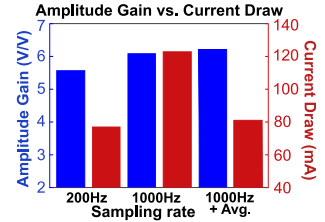


Figure 10: Power reduction with OAA.

6 SIGNAL PROCESSING

6.1 WAKE On-board signal processing.

Adaptive Gain Control. As aforementioned in Sec. 5, one important and unique challenge in ensuring high fidelity BTE signals is the large difference in the amplitude range (which could be up to three orders of magnitude) between EEG/EOG and EMG signals. Thus, the analog gain of our sensing circuit needs to adapt dynamically with the changes in signal amplitude. Fortunately, we observe that (1) EMG events do not happen frequently, (2) EMG events can happen quickly with strong amplitude changes, and, (3) signal amplitude during an EMG event is stochastic and can vary significantly. Understand these characteristics, we then design our AGC to (1) keep the gain at maximum for EEG/EOG signals while there is no significant EMG events, (2) react quickly to the abrupt increase of amplitude to detect EMG events but (3) react slowly to the decrease of amplitude while an EMG event is still happening to avoid gain oscillation. Peak Envelope (PED) and Square Law (SLD) detectors are two popular AGC techniques [68, 112] that fit with our needs. We use PED because of its low computational complexity. If there is no EMG event, we use a small window size so that PED can react quickly while a larger window size is used during an EMG event to avoid gain oscillation. AGC is implemented right after oversampling in the sensing circuit firmware to ensure its fast response. We interpolate missing samples with light-weight linear interpolation. Fig. 9 shows an EMG event could be captured without saturation with AGC.

Oversampling and Averaging (OAA). Low power usage is one important factor for a wearable device. To ensure high signal quality while being power efficient, we employ oversampling locally on the sensing circuit and down-sampling by taking the average of the collected samples before sending out the average values. OAA has been shown to improve signal quality by reducing the effect of random noises [61]. In WAKE, noise sources such as thermal noises, variations in voltage supply, variations in reference voltage, ADC quantization noises could be considered random noises [61] and are reduced with OAA. In addition, oversampling also helps our AGC to react faster to signal changes.

6.2 WAKE Physiological Signals Extraction

In WAKE, each sensor data (EEG/EOG/EMG, and EDA) is pre-processed at the host device corresponding to their own characteristics before putting it into the signal analyzing procedure. We show the examples of changes in those signals between microsleep and awake states in Fig. 11. We apply to all sensor data the notch filter

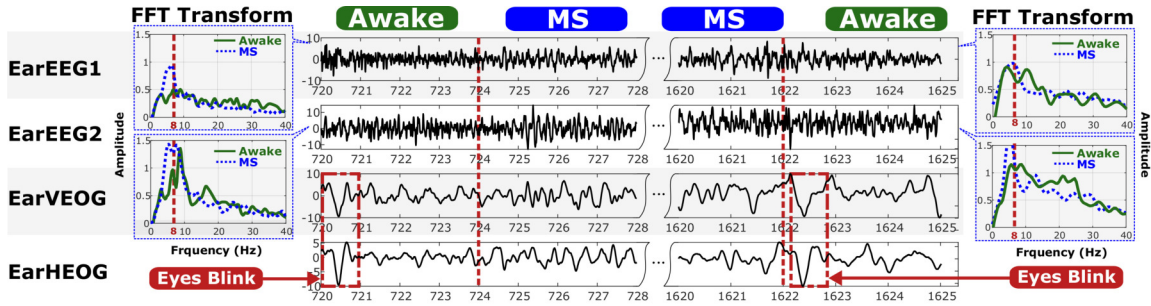


Figure 11: Signals captured by WAKE during the transition between awake and microsleep.

to remove 50/60Hz power line interference, linear trend removal to avoid DC drift, and outlier filters to remove spikes and ripples.

Collecting EEG/EOG/EMG signals. WAKE’s mixed-biosignals include EEG, EOG, and EMG, which are in the frequency range of 4-35 Hz, 0.1-10 Hz, and 10-100 Hz respectively [48]. We apply different bandpass filters to split the mixed BTE biosignals into the signals at the frequency range of interest. In particular, we extract wakefulness-related EEG bands (i.e. θ , α , and β waves) using 4-8 Hz, 8-12 Hz, 12-35 Hz bandpass filters, respectively. We extract horizontal EOG (hEOG) for eye movement and vertical EOG (vEOG) for eye blink using 0.3-10 Hz filters [69]. A 10-100Hz bandpass filter and a median filter are then applied to the mixed signals to extract the EMG band and get rid of spikes and other excessive components.

Collecting EDA signal. EDA signal is the superposition of two different components, skin conductance response (SCR) and skin conductance level (SCL) at the frequency range of 0.05-1.5 Hz and 0-0.05 Hz, respectively [124]. Even though EDA signals have fast responses, they are very slow to decline to baseline. Thus, if another response happens right after the first response, the signal level will increase even more [4]. Thus, frequency filtering is not effective to separate EDA signal. To address this, we employ a non-negative deconvolution technique proposed in [5] to decompose EDA into SCR and SCL components.

7 ALGORITHMS

EMG active events detection: Microsleep appears when the body is relaxed. A strong EMG signal can have significant power across all frequency bands of interest (discussed in Sec. 3). It will contaminate our BTE EEG and EOG signals rendering them unusable. We detect the active event based on the sum of all frequency bands in the spectrogram. For each data signal, we use the first 10 seconds as the ground-based noise. Any data whose total spectrum energy is 10% larger than that of ground-based is an active event.

Feature Extraction: We divide the collected time series data from each source into fixed-size epochs. Then, selected features are extracted from each epoch to be used for classification.

Temporal features: This category includes typical features used in the literature for time series data analysis in the temporal domain, namely mean, variance, min, max, hjorth, skewness, and kurtosis. In microsleep detection, EOG, EMG, and EDA signals are often analyzed in the time domain due to their considerable variation in amplitude and lack of distinctive frequency patterns [84]. Those six temporal features are extracted from each of hEOG, vEOG, EMG, and EDA signals for a total of 24 temporal features. We use wavelet decomposition for the hEOG signal to extract saccade features [115],

namely mean velocity, maximum velocity, mean acceleration, maximum acceleration, and range amplitude. Eyeblink features [69], namely blink amplitude, mean amplitudes, peak closing velocity, peak opening velocity, mean closing velocity, and closing time are extracted from the vEOG signal.

Spectral features: The spectral features are extracted to analyze the characteristics of the EEG signal because brainwaves are generally available in discrete frequency ranges at different stages [52]. Those features include the ratio of powers, absolute powers, θ/β , α/β , θ/α , and $\theta/(\beta+\alpha)$. Accordingly, 14 features are extracted from each channel of EEG providing 28 spectral features in total.

Non-linear features: Bioelectrical signals show various complex behaviors with nonlinear properties. In particular, the chaotic parameters of EEG can be used for microsleep detection. The discriminant ability of nonlinear analyses of EEG dynamics is demonstrated through the measures of complexity such as correlation dimension, Lyapunov exponent, entropy, fractal dimension, etc. [62], with the last two features proven to be most informative. In this study, we extract these two non-linear features for each of the two EEG channels (a total of four features).

Feature Selection: When all features are used altogether, irrelevant correlated features or feature redundancy can degrade the performance. Therefore, we adopt three feature selection methods, including Recursive Feature Elimination (RFE), L1-based, and tree-based feature selection to select the set of most relevant features out of 76 of them. RFE [15] is a greedy optimization algorithm that removes the features whose deletion will have the least effect on training error. L1-based feature selection [65] is used for linear models, including Logistic Regression and SVM. In our linear models, we use the L1 norm to remove features with zero coefficients. Finally, the feature importance ranking generated by the tree-based model [30] is used for eliminating the irrelevant descriptors.

Microsleep Classification: Various classification methods from Support Vector Machine (SVM), Linear Discriminant Analysis (LDA), Logistic Regression (LR), Decision Tree (DT) to ensemble methods like RandomForest or AdaBoost have been proposed in the literature for awake and microsleep classification, each shown to be effective in specific settings [59, 98]. To cope with the high complexity of our collected signals, we developed a hierarchical stack of three base classifiers. Our hierarchical model consists of a Random Forest classifier (with 50 estimators) in the first layer, Adaboost classifier (with 50 tree estimators) in the second layer, and SVM (with RBF kernel) in the last layer. Specifically, for the first two layers, we only keep the predictions with high probabilities (> 0.7) and transfer the rest of samples to the next layer. In the last layer, SVM classifies all

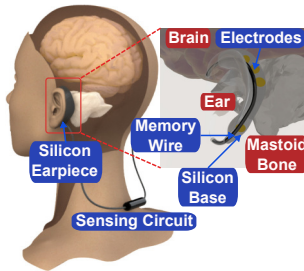


Figure 12: 3D model.

of the remaining samples. We also apply a heuristic rule to the final predication based on the knowledge that an EMG event is likely to leads to an 'awake' event. The results of our empirical analysis are presented in Sec. 9, which highlights the overall accuracy of the performance and proves the efficiency of the proposed classification model. In our experiments, subjects that were inevitably awake all or most of the time during data collection caused the significant imbalance between the classes versus 'awake'. To overcome this problem, we first remove the data of all sessions where subjects never entered microsleep. Then, we apply under-sampling to the awake samples to avoid under-learning for microsleep class.

8 IMPLEMENTATION

Earpieces' material. We design the BTE biosensing earpieces by attaching electrical conductive material on top of a silicone base as illustrated in Fig. 12. The silicone material (Dragon Skin 10) is chosen so that the earpiece can fit with the curve created by the mastoid bone behind the ears, while being comfortable and alterable with different user's ears (Fig. 12). Furthermore, the chosen silicone material is skin safe and does not create irritation to the user's ears. The silicone base is molded based on the average size of the human ear (the average ear is around 6.3 centimeters long and the average ear lobe is 1.88 cm long and 1.96 cm wide [106, 110]). To maintain a good contact between the electrodes and skin, we put a memory wire core inside the silicone base. The memory wire core creates a grip on the wearer's ears, pushing the silicone against the skin. Furthermore, it also helps the earpieces be usable for different human ear sizes and shapes (Fig. 13).

Electrodes' material. We evaluated three different materials for the electrodes attached to the earpieces including (1) silver fabric, (2) copper pad and (3) gold-plated copper pad. The silver fabric electrodes are highly conductive and can make good contact with the skin thanks to the flexibility of the fabric, but the silver gets tarnished quickly because of the skin oil and sweat. Thus, the contact quality degrades after several uses as the resistance increases dramatically from less than 1Ω to several hundred $k\Omega$. Similarly, copper-based electrodes also degrade quality after several uses. We address that issue by plating gold liquid over the copper electrodes, because the gold-plated electrodes are more resistant to skin oil and sweat. In addition, gold is well-known to be chemically inert. Thus, the skin allergy with gold is extremely rare [91]. The resistance of the gold-plated electrodes is always less than 1Ω . To enhance contact conductivity and adhesion, we apply Weaver's Ten20 conductive paste [118] on the electrodes before wearing the earpieces. The contact impedance between the electrodes and the skin is also measured to be in the range from 5 to 10 $k\Omega$ at 30Hz with

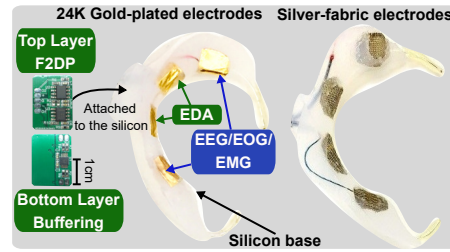


Figure 13: BTE silicon earpieces.

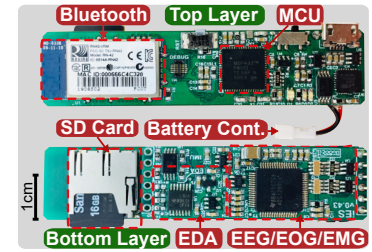


Figure 14: WAKE circuit.

a proper skin preparation. This contact impedance value satisfies the clinical standards [13, 101], which state the acceptable upper limit is $10k\Omega$, to achieve optimal biosignals recording.

■ Putting Things Together.

We use the low power, precision AD8244 input buffer to implement our Stage 1 of 3CA. The AD8244 device has unity gain, very high input resistance (i.e., $20T\Omega$), and very low input capacitance (i.e., $12pF$) so that the effect of electrode fluctuation can be minimized as pointed out in Eq. 3. The precision, dual-channel instrumentation amplifier AD8222 is used to implement our Stage 2 (F2DP). The preamplifying gain is chosen at 100 so the full range of the ADC (i.e., $-2.5V$ to $2.5V$) is utilized. We use ultra-low noise integrated amplifiers and 24-bits ADC chip ADS1299 ($1\mu V$ peak-to-peak internal noise) to digitize the signals. OAA is implemented by oversampling the signals 10 times the maximum frequency of interest (i.e. 100Hz). The downsampling ratio by averaging is 5. It yields the final sample rate at 200Hz for the signals to be transmitted over Bluetooth. Furthermore, we measure the skin-electrode contact impedance (Contact-Z) (at 250Hz) to determine whether an electrode is making good contact with the skin or not and notify the user so they can adjust. The main processing unit (MSP432) is used to (1) drive the analog front end on the sensing circuit, (2) to adjust the amplifier gain dynamically, and (3) to stream data to a host device through Bluetooth. Note that all components are configured to operate at low power (Bluetooth transmission and SD Card consume at maximum 45 mA and 100 mA, each amplifier in our analog front end circuit and the MCU consume at maximum around 10 mA or less.)

9 PERFORMANCE EVALUATION

9.1 BTE Signals Sensitivity Validation

In this section, we compare the ability to capture EEG, EOG, EMG, and EDA with WAKE from BTE against the ground-truth devices from standard placements on the scalp, the eyes, the chin, and the wrist (Fig. 3). Ground-truth EEG, EOG, and EMG are measured by using an FDA-approved Lifeline Trackit Mark III device with electrodes placed at C3, C4, O1, O2, Cz, M1, M2, upper and lower parts of the left eye (VEOG), two sides of the left and right eyes (HEOG), and the chin (chinEMG), according to the International 10-20 system [53]. Ground-truth EDA is measured by the BioPac's BioNomadix Wireless EDA Amplifier system with electrodes placed on the left wrist. The data was collected for one hour while the subject sat on a couch. We calculate Normalized Cross-Correlation (NCC)[66] between our BTE signals with the ground-truth ones to measure the similarity between them. The measured signals are shown in Fig. 15. NCCs of EEG, EOG, EMG, and EDA are as follows:

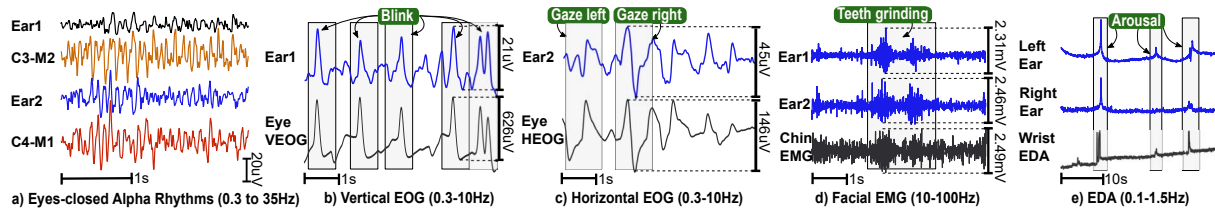


Figure 15: BTE EEG, EOG, EMG and EDA signals vs. ground-truth.

Ear1-C3: 0.35, Ear1-O1: 0.28, Ear2-C4: 0.44, Ear2-O2: 0.52, Ear1-VEOG: 0.47, Ear2-HEOG: 0.59, Ear1-chinEMG: 0.62, Ear2-chinEMG: 0.76, and EarEDA-WristEDA: 0.37. The results show that Ear2, i.e. the channel crossing right and left ears, has strong correlations with scalp EEG and horizontal EOG. Ear1, i.e. the channel placed on the left ear, has a moderate correlation with scalp EEG and a strong correlation with vertical EOG. Both Ear1 and Ear2 channels have strong correlations with chin EMG. EDA on the left ear shows a moderate correlation with the signal from the wrist.

9.2 Noise Suppression Performance

Motion Artifacts Mitigation. We evaluated the 3CA technique in two scenarios: (1) walking and (2) sitting in a car. Each evaluation is done in one hour. Evaluation (1) consists of ten minutes of standing stationary and 50 minutes of walking in a hallway. Evaluation (2) also consists of ten minutes of sitting in a car while it is parked in a parking lot and 50 minutes of driving on an urban road (40 mph). Evaluation (1) presents artifacts created by human motion while evaluation (2) presents artifacts introduced from the environment while driving. Two pairs of electrodes are put as close as possible on the same ear of a subject so that the same signals could be obtained.

Without 3CA, the BTE EOG signals (i.e. eye blinks) are completely distorted by significant motion artifacts. The noise power introduced by motion is shown in Fig. 19. During standing and parking scenarios, BTE signals with and without 3CA have the same power. However, during walking and driving, 3CA reduces the noise power by 19.47 dB and 11.87 dB. Thus, the eye blink signals are captured reliably (Fig. 17, 18).

Environmental Noise Reduction. We evaluated the ability to minimize environmental noise in three different practical environments: (1) in an office, (2) at home, and (3) inside a car. The results of the noise spectrum are shown in Fig. 20, 21, and 22, where 3CA can reduce the noise power by 9.74 to 16.1 dB. We also found that the 60Hz noise and its harmonics coupled from the electrical power line are the main sources of noise while the subject is stationary. However, during motion, motion artifacts are the most significant noise source at frequency ranges 0.3-100Hz (Fig. 22).

9.3 Microsleep Detection Performance

We evaluated WAKE's ability to detect microsleep by conducting the Maintenance of Wakefulness Test (MWT), which is the existing gold-standard for quantifying microsleep [1, 107]. We conducted three sets of experiments on the data of 19 subjects. In the first experiment, we performed the Leave-One-Subject-Out Cross-Validation (LOSOVCV), i.e. train each classifier on the set of 18 subjects and evaluate on the unseen subject. The second and third sets deal with each individual subject, in which we provided both Leave-One-Out Cross-Validation (LOOCV) and test-set evaluations.

Table 1: Demographic data of participants

Age	18 - 44 years old
Sleepiness Level	Healthy: 9, EDS: 8, SEDS: 1, Narcolepsy: 1
Gender Ratio	Male: 12, Female: 7

Experimental Protocol. WAKE protocol has been thoroughly designed and approved by the Institutional Review Board (IRB). 19 sleep-deprived and narcoleptic subjects on the campus were recruited for the study. Participants' demographics are shown in Tab. 1. The Daytime Sleepiness Level of each subject was recorded by using the Epworth Sleepiness Scale (ESS) [56]. The ESS score is interpreted as <10, healthy level; 10-15, Excessive Daytime Sleepiness (EDS); and 16-24, Severe Excessive Daytime Sleepiness (SEDS). The subjects were advised to sleep for less than five hours (only applied to subjects at the healthy level) on the night before the study and also not to consume caffeine or alcohol products before doing the study so that their microsleep could be faithfully captured. During each MWT session, the subject was asked to try to stay awake in a sleepiness-inducing environment. We use an FDA-Approved Ambulatory video-EEG system (Lifelines Trackit Mark III) to conduct PSG as the 'ground truth'.

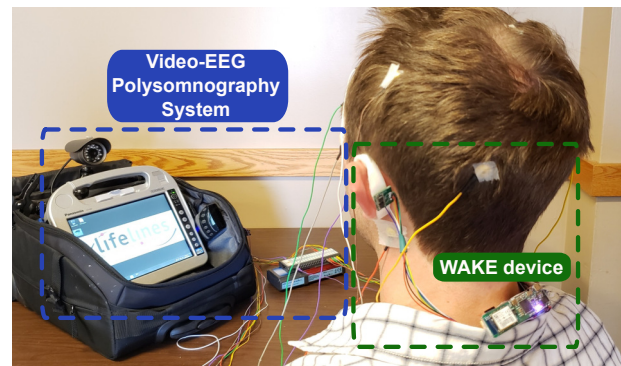


Figure 16: Experiment setup.

The MWT Protocol. We conducted two sessions of MWT for each subject with a maximum of 40 minutes each. The subject was asked to sit comfortably on a couch. The WAKE device and the 'ground-truth' PSG system were installed on them as shown in Fig. 16. We minimized all the external factors that could affect the subject's drowsiness by blocking all the light and sound coming from outside of the experiment room. The room was dark and its temperature was set at the subject's comfort levels. The subject was asked to relax but try to keep themselves awake for as long as possible, so they would not fall asleep voluntarily. The MWT starts

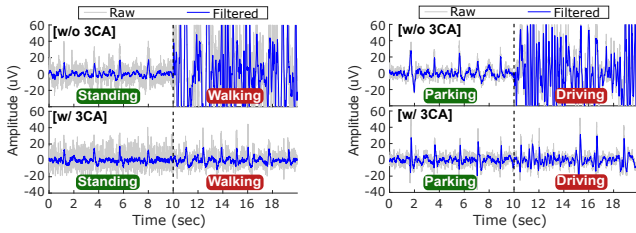


Figure 17: Walking motion noise suppression.

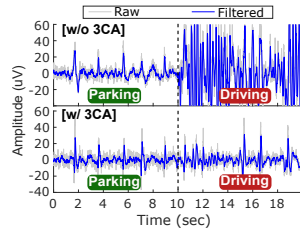


Figure 18: Driving motion noise suppression.

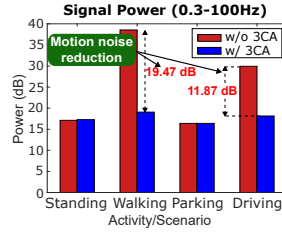


Figure 19: Motion noise power reduction.

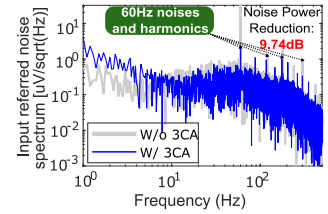


Figure 20: 3CA noise reduction (In an Office).

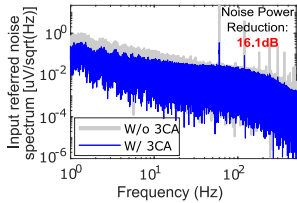


Figure 21: 3CA noise reduction (At Home).

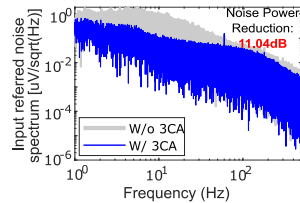


Figure 22: 3CA noise reduction (Inside a Car).

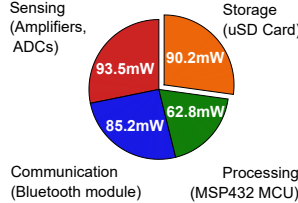


Figure 23: Active power usage breakdown.

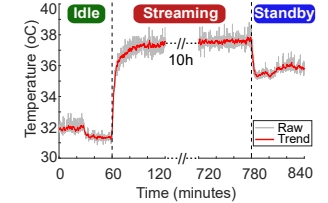


Figure 24: CPU core thermal profile.

when the light in the experiment room was turned off. We woke the subject up after they fell asleep. The collected PSG data was sent out for scoring by two certified sleep experts. To handle the variation of the manual process, one expert scored while the other expert verified independently, and the differences were resolved by discussion. Awake and microsleep episodes were marked down by following the guideline of AASM for Sleep Study [48].

Table 2: Classification results (epoch=5s)

Experiment	Precision	Recall (Sensitivity)	Specificity
Set 1 - LOSOCV	0.76	0.85	0.85
Set 2 - Test-set	0.87	0.9	0.96
Set 3 - LOOCV	0.88	0.89	0.96

■ Classification Model Performance.

Classification Evaluation Metrics. We cast the problem of microsleep detection as a binary classification problem: positive class for microsleep epoch and negative class otherwise. Here, we briefly describe four indices of the confusion matrix: true positive (TP) is the number of actual positive epochs which are correctly classified; true negative (TN) is the number of actual negative epochs which are correctly classified; false positive (FP) is the number of actual negative epochs which are incorrectly classified as positive; false negative (FN) is the number of actual positive epochs which are incorrectly classified as negative. Given these notions, we can now define precision, recall (sensitivity), specificity scores as follow:

$$\text{Precision} = \frac{TP}{TP + FP}; \quad \text{Recall} = \frac{TP}{TP + FN}; \quad \text{Spec.} = \frac{TN}{TN + FP}$$

Due to the nature of our detection problem (the number of microsleep epochs is much less than that of awake ones), precision, recall, and specificity are preferred over the accuracy index.

Data summary. Our data consists of 35,558 and 8,845 samples of 5s-epoch (80% overlap) for awake and microsleep states, respectively. The ratio of negative:positive is approximately 4:1, as an essence of rare microsleep events. This imbalance problem is known

to severely affect the performance of popular classification algorithms. Thus, we downsampled the awake set to the same amount of microsleep data in each experiment and put this imbalance ratio (number of negative epochs/number of positive epochs) in the weighted cost during training. For instance, in the first iteration of the LOSOCV experiment, we left subject 18 out for testing and we pooled samples of all training subjects, which consists of 32,778 negative samples and 8,572 positive samples. We downsampled the negative samples to 8,572 instances (same as the positive one) and used the weighted cost of 32,778:8,572 for training.

Set 1: Leave-one-subject-out cross validation: we alternatively trained our classifiers on the data pool of 18 subjects and evaluated the trained model on the remaining subject. The final scores are the average over these 19 iterations. The hierarchical classifier achieved the best performance among examined classifiers, with 0.76, 0.85, and 0.85 for precision, recall, and specificity, respectively. This result was expected since there exists slight value-shifts across the subjects. Nevertheless, this result shows the feasibility of WAKE for microsleep detection on unseen subjects.

Set 2: Test-set on each subject (Test-set): we applied stratified split into the data set of each subject into two parts as the ratio 75% (training): 25% (testing) with respect to the percentage of positive and negative samples. We then trained our classifiers on the training data and evaluated the performance on the test set. Among simple classifiers, RandomForest model achieved the best scores with a precision of 0.87, a recall of 0.9, and 0.96 for specificity.

Set 3: Leave-one-out cross validation: we conducted LOOCV for each subject’s data and averaged the scores for the final results. Specifically, for LOOCV on a particular subject, we left one epoch for evaluation and trained on the remaining data. This procedure was performed N times (N is the size of that subject’s data) before we got the average scores as the representative. This approach is especially suitable for small sample-size subjects. The Random Forest classifier was able to achieve an average precision, recall, and specificity of 0.88, 0.89, and 0.96, respectively, over all of the subjects. Tab. 2 shows the classification results of the experiments.

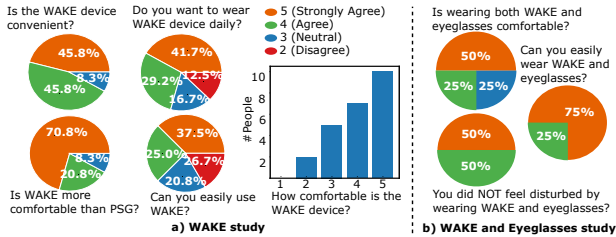


Figure 25: User study.

9.4 Usability Analysis

WAKE Prototype Power Usage. We measured the power consumption of the WAKE prototype by using a Monsoon Power Monitor device [49] with the sampling rate at 5 kHz. Each measurement was done in 180s, resulting in 900k data points, to get a stable result. At 25°C and 3.7V nominal battery voltage, the average power usage of WAKE is as follows: (1) Active state (real-time biosignals streaming with Bluetooth) consumes 241.5mW, and (2) Idle state (no streaming with only MCU is kept running in idle mode while other components are turned off) consumes 51.60mW. With a 600mAh Li-Po battery, WAKE prototype can remain operation for 9.2 hours in Active, and stay in Idle for 43.1 hours. Further component-level measurements of usage power during Active were done by turning off each component one by one and repeating the measurements. Fig. 23 presents a full active power usage breakdown of the WAKE device. The sensing components (amplifiers and external ADCs) and Bluetooth communication module consume the most of system power with the average of 93.5mW and 85.2mW, respectively. The storage module (uSD card) will increase an additional 90.2mW if it is turned on. The processing unit (MSP432 MCU) only consumes 62.8mW. These numbers show the capability of our WAKE prototype to monitor the user’s microsleep during a long duration. They could be further lowered by reducing the number of sensing components, optimizing Bluetooth transmission parameters, and taking advantage of deep power saving modes of the MCU.

WAKE Prototype Thermal Profiling. We conducted thermal measurement for the processing unit of our WAKE prototype for 14 hours continuously. The measurement was designed to emulate the scenario where continuous microsleep monitoring is needed during normal working hours. It was divided into three states: (1) idle (the device waits for a Bluetooth connection), (2) streaming (the device streams the measured biosignals to both its onboard uSD Card and a Bluetooth-connected mobile device), (3) standby (the device stops data streaming but its Bluetooth connection is still available for future commands). The idle, streaming, and standby states lasted for 1, 12, 1 hour, respectively. Thermal data was measured by the internal temperature sensor of the processing unit and reported every 5s. Fig. 24 presents our measurement results. On average, the temperature of idle and standby states are 31.65 and 35.75 degrees Celsius, respectively. During streaming, the temperature increases to an average of 37.38 degrees and the peak is 38.9 degrees. According to the standard of American Society for Testing and Materials, 43 degrees Celsius is the threshold for prolonged use (i.e. >8h) on human skin without creating any injury [17, 25, 44]. The temperature of our WAKE prototype is always below this threshold.

User Study. We conducted a survey to evaluate WAKE’s usability. We distributed our survey to the 19 subjects in our MWT study

and 17 other people on the campus after they have used the WAKE device for at least two hours. In total, 36 people answered our survey. Fig. 25a presents the questions that we used to ask our participants’ opinions on their experience with the WAKE device. The results show that over 85% of people felt comfortable with our WAKE device and were willing to wear it during daily mental fatigue tasks, such as during driving, night-time working, etc. 91.6% of people agree that the WAKE device is more comfortable than the ‘ground-truth’ device used in PSG. 62.5% of people found it easy to use the WAKE device, while 16.7% had some difficulties with skin preparation and putting on the conductive paste.

We noticed that people with eyeglasses are most likely to be affected by wearing WAKE, as both devices need to be rested on users’ ears. Thus, to evaluate the compatibility of WAKE and eyeglasses during daily activities, an additional users’ study on a population of eight people was conducted. In this study, we asked the users to wear both WAKE and eyeglasses during their daily working time for 3-4 hours. They were asked to wear WAKE before wearing eyeglasses so that the eyeglasses’ temple tips could sit on top of the WAKE’s silicone earpieces. The survey questions and results are presented in Fig. 25b. All users reported that they did not feel disturbed during their normal activity, and they can easily wear both WAKE and eyeglasses. 75% of users agree that it was comfortable to wear both devices for long hours thanks to the softness of the silicon. Only two users had slight discomfort because of additional weight and the gripping force of WAKE earpieces.

10 RELATED WORKS

Existing microsleep detection systems mainly use scalp EEG, eye tracking with EOG or cameras, IMU, and infrared light. EEG and EOG signals have been widely used to detect microsleep [12, 27, 28]. However, the conventional devices used to capture those signals can only be used in a controlled environment and are not socially acceptable. Camera-based approaches detect microsleep by analyzing the movement of head and eyes [97, 104, 125], face [117], pupil [6] or iris [22]. Although blinks and saccades detected by image processing have been shown to monitor the appearance of microsleep, detection of microsleeps occurred too late during the driving simulation [97]. IMU sensors can be used to approximate body motion corresponding to microsleep (smartwatch [64], hair-band [117]). In addition, infrared light reflection methods monitor the eyelid movement of the subject such as Vigo [116], BlinQ [10]. These devices cannot recognize the inner physiological state and its reliability has not been thoroughly evaluated.

In literature, there are also many drowsiness detection and monitoring works such as [58, 67, 93]. Drowsiness and microsleep detection works, however, should not be treated equally. In particular, drowsiness is a physiological state that is defined when there exists a sleep pressure, which may cause slower reaction time or compromise vision but does not mean fatal as our brain is still conscious of the surrounding environment [40, 92]. Microsleep, on the other hand, is the brief and often fatal duration, where the brain loses consciousness [45]. Additionally, drowsiness detection works (especially in driving scenarios) use various methods to quantify the existence of drowsiness such as steering pattern monitoring, vehicle position in lane monitoring, driver eye/face monitoring, etc. [93], which are different from ones (i.e. brain activity represents

microsleep period) used for microsleep. Particularly, in [58], the authors detect drowsiness by quantifying wake/sleep epochs, however, they also state that their system is not sensitive enough to detect microsleep events. In [67], lane deviation in a driving simulation, which is pointed out in [93] that it is not a reliable metric, is used as the indicator of drowsiness.

In-ear sensing system for EEG signals is particularly useful for sleep monitoring like LIBS [77], Hearables [29], ear-eeg [60, 72, 74]. However, wearing the device inside the ear might impact hearing capability and user daily activities. cEEGrids [9] and Gu et al. [37] compared scalp EEG with behind-the-ear EEG and demonstrated that EEG data can be recorded behind the ear. However, the ability to detect microsleep from BTE has not been evaluated before. Vital signs monitoring using wearable and mobile sensors has also been investigated in various studies such as breathing measurement [75], tongue-teeth localization (EEG, EMG, and skin surface deformation) [78], stress estimation (heart rate variability (HRV), galvanic skin response, and EMG) [120], mental health management (EEG, hemoencephalography, and HRV) [42], and eating detection (IMU, microphone, and proximity sensor) [3, 8]. However, to the best of our knowledge, there are no existing works to detect microsleep from wearable BTE sensors accurately and reliably.

11 DISCUSSIONS

In-the-wild evaluation. With the promising results from our in-lab evaluation, we aim for a larger scale out-lab evaluation. One of the key challenges is the limitation of the existing ground-truth for microsleep detection. Up to now, the gold standard to objectively assess microsleep is based on polysomnographic (PSG) data, which can only be conducted in a controlled environment [102]. Ground-truths based on pupil dilation or eye-tracking have potentials and are directions worth exploring.

Impact of sweat condition. While WAKE can address motion and environmental noises, there are several artifacts posing as challenges to the real-world usability of a wearable system like WAKE. For instance, sweating and hydration can introduce noises into the measurement. Addressing these artifacts is the question that we will explore to enhance the practicality of WAKE.

Optimizing WAKE device. The current prototype is designed with general-purpose off-the-shelf materials and components. Hence, it is challenging to ensure the manufacturing quality of our customized earpieces, electrodes, and the sensing circuit. The WAKE earpieces are designed in two sizes (i.e. normal and small) to address the difference in ears' sizes among people. However, we still need to rely on the conductive paste and gripping force of the earpieces to address the gap between the electrodes and the user's skin. The use of wet electrodes in our current design is also not desirable during daily usages because of the additional steps needed to apply the conductive paste. Additionally, The current power consumption is still high. Thus, improving the quality of our customized components, optimizing power consumption, employing dry electrodes, and a better mechanism to maintain electrode-skin contact are important tasks to further increase the usability of the system.

Trade-off between classification performance and latency. To significantly improve the performance of classification, ones usually make use of more complicated algorithms (e.g. deep neural networks) or extract more complex features, thus probably resulting

in the increase of the prediction time. This can be seen as a trade-off between the accuracy and latency, and a careful reader may question on how to optimize the balance point. Being aware of this trade-off, we focus on improving the inference (high accuracy) using well-studied and simple classifiers (e.g. logistic regression, random forest) because they are commonly deployed and optimized in latency-sensitive services and libraries. Furthermore, our features are highly selected based on expert's knowledge, so that they are not only informative but also simple and efficient to compute. Hence, these settings help our system to achieve a small processing and prediction time (approximately 0.1ms for each epoch), shortening the latency toward warning the user.

Microsleep epoch size. Another factor affecting the latency and accuracy of our system is the epoch size, which is chosen as 5s from the advice of our sleep experts and based on previous study [12, 27]. Specifically, [12] points out that epoch size can vary between 4 and 10s without any degradation while the other study [27] points out that 5s epoch yields the best detection accuracy. Too short epochs may prevent optimal features to be extracted from the signals. With a 5s epoch setting, our model shows a good prediction accuracy with a reasonably low detection latency, which probably indicates an optimal point on the Pareto curve of latency and accuracy.

Potential use cases and warning systems. WAKE has the potential to prevent microsleep-related accidents and hazards during daily activities of factory and night-shift workers, drivers, pilots, sailors, etc. Furthermore, WAKE's ability to monitor human cognitive states and behaviors can enable various wearable solutions to address the challenges of epileptic seizures, focus, autism, etc.

Warning systems based on light, sound, and vibration are widely employed in literature and commercialized systems [6, 23, 31, 71, 116]. They could be easily integrated with WAKE to provide warnings to the users. Furthermore, recent advancements in non-invasive brain stimulation techniques [34, 35] could provide a new direction on preventing microsleep without the need for a warning alarm.

12 CONCLUSION

We presented WAKE, a novel compact, lightweight, and socially acceptable wearable device to detect microsleep from behind the ears. We proposed the Three-fold Cascaded Amplifying technique to remove the impact of motion artifacts and environmental noises. We evaluated the motion and environmental noise suppression and microsleep detection performance on 19 subjects. WAKE can reduce noise power by 9.74 - 19.47 dB in different practical scenarios such as walking, driving. We develop a classification model based on the core biomarkers of microsleep captured by WAKE. WAKE achieves 76% precision and 85% recall in detecting microsleep in LOSOCV.

ACKNOWLEDGEMENTS

We thank our shepherd, Dr. Rijurekha Sen, and anonymous reviewers for their insightful comments on the manuscript. We also would want to thank Ms. Carole Kline, Dr. Scott Holman, Vachan D A, Frederick Thayer, Evan Stene, Anh Nguyen, and Katrina Siegfried for your valuable supports with the project. This research was partially funded by NSF CNS/CSR #1846541, NSF SCH #1602428.

REFERENCES

- [1] A. M. Annis, A. Young, and D. M. O'Driscoll. Importance of urinary drug screening in the multiple sleep latency test and maintenance of wakefulness test. *Journal of Clinical Sleep Medicine*, 12(12):1633–1640, 2016.
- [2] G. Ballou. *Handbook for sound engineers*. Taylor & Francis, 2013.
- [3] A. Bedri, R. Li, M. Haynes, R. P. Kosaraju, I. Grover, T. Prioleau, M. Y. Beh, M. Goel, T. Starner, and G. Abowd. Earbit: using wearable sensors to detect eating episodes in unconstrained environments. *Proceedings of the ACM on interactive, mobile, wearable and ubiquitous technologies*, 1(3):37, 2017.
- [4] M. Benedek and C. Kaernbach. A continuous measure of phasic electrodermal activity. *Journal of neuroscience methods*, 190(1):80–91, 2010.
- [5] M. Benedek and C. Kaernbach. Decomposition of skin conductance data by means of nonnegative deconvolution. *Psychophysiology*, 47(4):647–658, 2010.
- [6] L. M. Bergasa, J. Nuevo, M. A. Sotelo, R. Barea, and M. E. Lopez. Real-time system for monitoring driver vigilance. *IEEE Transactions on Intelligent Transportation Systems*, 7(1):63–77, 2006.
- [7] S. Berman, J. O'Neill, S. Fears, G. Bartzokis, and E. D. London. Abuse of amphetamines and structural abnormalities in the brain. *Annals of the New York Academy of Sciences*, 1141(1):195–220, 2008.
- [8] S. Bi, T. Wang, N. Tobias, J. Nordrum, S. Wang, G. Halvorsen, S. Sen, R. Peterson, K. Odam, K. Caine, et al. Auracle: Detecting eating episodes with an ear-mounted sensor. *Proceedings of the ACM on Interactive, Mobile, Wearable and Ubiquitous Technologies*, 2(3):1–27, 2018.
- [9] M. G. Bleichner and S. Debener. Concealed, unobtrusive ear-centered eeg acquisition: ceegrids for transparent eeg. *Frontiers in human neuroscience*, 11:163, 2017.
- [10] BlinQ. Blinq system. <https://tinyurl.com/yxlkcsr5>. [Online; accessed Mar 28, 2019].
- [11] W. A. Broughton and R. J. Broughton. Psychosocial impact of narcolepsy. *Sleep*, 17(suppl_8):S45–S49, 1994.
- [12] A. B. Buriro, R. Shoorangiz, S. J. Weddell, and R. D. Jones. Predicting microsleep states using eeg inter-channel relationships. *IEEE Transactions on Neural Systems and Rehabilitation Engineering*, 26(12):2260–2269, 2018.
- [13] T. P. R. Center. Procedure manual for polysomnography. <https://tinyurl.com/y9p9tdjz>. [Online; accessed Apr 21, 2020].
- [14] A. A. Centers. *Narcolepsy and How Substance Abuse Effects It*, 2018. <https://americanaddictioncenters.org/co-occurring-disorders/narcolepsy>.
- [15] X. Chen and J. C. Jeong. Enhanced recursive feature elimination. In *Sixth International Conference on Machine Learning and Applications (ICMLA 2007)*, pages 429–435, Dec 2007.
- [16] Y. M. Chi and G. Cauwenberghs. Wireless non-contact eeg/ecg electrodes for body sensor networks. In *2010 International Conference on Body Sensor Networks*, pages 297–301. IEEE, 2010.
- [17] I. E. Commission. Electrotechnical equipment - temperatures of touchable hot surfaces. 2010.
- [18] N. S. Council. *Fatigue – You're More Than Just Tired*, 2019. <https://www.nsc.org/work-safety/safety-topics/fatigue>.
- [19] I. Daly, M. Billinger, R. Scherer, and G. Müller-Putz. On the automated removal of artifacts related to head movement from the eeg. *IEEE Transactions on neural systems and rehabilitation engineering*, 21(3):427–434, 2013.
- [20] D. Dawson, A. C. Reynolds, H. P. Van Dongen, and M. J. Thomas. Determining the likelihood that fatigue was present in a road accident: a theoretical review and suggested accident taxonomy. *Sleep medicine reviews*, 2018.
- [21] R. Dodel, H. Peter, T. Walbert, A. Spottke, C. Noelker, K. Berger, U. Siebert, W. H. Oertel, K. Kesper, H. F. Becker, et al. The socioeconomic impact of narcolepsy. *Sleep*, 27(6):1123–1128, 2004.
- [22] T. D'Orazio, M. Leo, C. Guaragnella, and A. Distante. A visual approach for driver inattention detection. *Pattern Recognition*, 40(8):2341–2355, 2007.
- [23] M. Flores, J. Armingol, and A. de la Escalera. Driver drowsiness warning system using visual information for both diurnal and nocturnal illumination conditions. *EURASIP journal on advances in signal processing*, 2010(1):438205, 2010.
- [24] R. Fog. Stereotyped and non-stereotyped behaviour in rats induced by various stimulant drugs. *Psychopharmacologia*, 14(4):299–304, 1969.
- [25] A. S. for Testing and Materials. Astm c1055 - 03 standard guide for heated system surface conditions that produce contact burn injuries. 2014.
- [26] P. M. Fuller, J. J. Gooley, and C. B. Saper. Neurobiology of the sleep-wake cycle: sleep architecture, circadian regulation, and regulatory feedback. *Journal of biological rhythms*, 21(6):482–493, 2006.
- [27] M. Golz, A. Schenka, F. Haselbeck, and M. P. Pauli. Inter-individual variability of eeg features during microsleep events. *Current Directions in Biomedical Engineering*, 5(1):13–16, 2019.
- [28] M. Golz, D. Sommer, M. Holzbrecher, and T. Schnupp. Detection and prediction of driver's microsleep events. In *Proc 14th Int Conf Road Safety on Four Continents*, volume 11. Citeseer, 2007.
- [29] V. Goverdovsky, W. von Rosenberg, T. Nakamura, D. Looney, D. J. Sharp, C. Papavasiliou, M. J. Morrell, and D. P. Mandic. Hearables: Multimodal physiological in-ear sensing. *Scientific reports*, 7(1):6948, 2017.
- [30] K. Grabczewski and N. Jankowski. Feature selection with decision tree criterion. page 6 pp., 12 2005.
- [31] R. Grace and S. Steward. Drowsy driver monitor and warning system. 2001.
- [32] H. Gray. *Gray's anatomy: with original illustrations by Henry Carter*. Arcturus Publishing, 2009.
- [33] S. L. Greene, F. Kerr, and G. Braitberg. Amphetamines and related drugs of abuse. *Emergency Medicine Australasia*, 20(5):391–402, 2008.
- [34] N. Grossman. Modulation without surgical intervention. *Science*, 361(6401):461–462, 2018.
- [35] N. Grossman, D. Bono, N. Dedic, S. B. Kodandaramaiah, A. Rudenko, H.-J. Suk, A. M. Cassara, E. Neufeld, N. Kuster, L.-H. Tsai, et al. Noninvasive deep brain stimulation via temporally interfering electric fields. *Cell*, 169(6):1029–1041, 2017.
- [36] B. Grundlehner and V. Mihajlović. Ambulatory eeg monitoring. 2019.
- [37] Y. Gu, E. Cleeren, J. Dan, K. Claes, W. Van Paesschen, S. Van Huffel, and B. Hunyadi. Comparison between scalp eeg and behind-the-ear eeg for development of a wearable seizure detection system for patients with focal epilepsy. *Sensors*, 18(1):29, 2018.
- [38] T. Guardian. *Google Glass security failings may threaten owner's privacy*. <https://www.theguardian.com/technology/2013/may/01/google-glass-security-privacy-risk>.
- [39] C. Guilleminault, M. Billiard, J. Montplaisir, and W. C. Dement. Altered states of consciousness in disorders of daytime sleepiness. *Journal of the neurological sciences*, 26(3):377–393, 1975.
- [40] C. Guilleminault and S. N. Brooks. Excessive daytime sleepiness: a challenge for the practising neurologist. *Brain*, 124(8):1482–1491, 2001.
- [41] J. T. Gwin, K. Gramann, S. Makeig, and D. P. Ferris. Removal of movement artifact from high-density eeg recorded during walking and running. *Journal of neurophysiology*, 103(6):3526–3534, 2010.
- [42] U. Ha, Y. Lee, H. Kim, T. Roh, J. Bae, C. Kim, and H.-J. Yoo. A wearable EEG-HEG-HRV multimodal system with simultaneous monitoring of tES for mental health management. *IEEE transactions on biomedical circuits and systems*, 9(6):758–766, 2015.
- [43] M. Hafner, M. Stepanek, J. Taylor, W. M. Troxel, and C. Van Stolk. Why sleep matters—the economic costs of insufficient sleep: a cross-country comparative analysis. *Rand health quarterly*, 6(4), 2017.
- [44] A. Q. Han. Thermal management and safety regulation of smart watches. In *2016 15th IEEE Intersociety Conference on Thermal and Thermomechanical Phenomena in Electronic Systems (ITherm)*, pages 939–944. IEEE, 2016.
- [45] L. Higgins and B. Fette. Drowsy driving. 2012.
- [46] J. Horne, L. Reyner, and P. Barrett. Driving impairment due to sleepiness is exacerbated by low alcohol intake. *Occupational and environmental medicine*, 60(9):689–692, 2003.
- [47] J. C. Huhta and J. G. Webster. 60-hz interference in electrocardiography. *IEEE Transactions on Biomedical Engineering*, 2(2):91–101, 1973.
- [48] C. Iber and C. Iber. *The AASM manual for the scoring of sleep and associated events: rules, terminology and technical specifications*, volume 1. American Academy of Sleep Medicine Westchester, IL, 2007.
- [49] M. S. Inc. Power monitor. <https://www.msoon.com/high-voltage-power-monitor>. [Online; accessed Apr 21, 2020].
- [50] T. Independent. *Google Glass will make 'privacy impossible' warn 'Stop The Cyborgs' campaigners*. <https://tinyurl.com/vphjxrv>.
- [51] Investopedia. *How and Why Google Glass Failed*. <https://www.investopedia.com/articles/investing/052115/how-why-google-glass-failed.asp>.
- [52] B. T. Jap, S. Lal, P. Fischer, and E. Bekiaris. Using eeg spectral components to assess algorithms for detecting fatigue. *Expert Systems with Applications*, 36(2, Part 1):2352–2359, 2009.
- [53] H. H. Jasper. The ten-twenty electrode system of the international federation. *Electroencephalogr. Clin. Neurophysiol.*, 10:370–375, 1958.
- [54] E. Jedari, R. Rashidzadeh, M. Mirhassani, and M. Ahmadi. Two-electrode eeg measurement circuit using a feed forward cmrr enhancement method. In *2017 IEEE 30th Canadian Conference on Electrical and Computer Engineering (CCECE)*, pages 1–4. IEEE, 2017.
- [55] P. Jennum, S. Knudsen, and J. Kjellberg. The economic consequences of narcolepsy. *Journal of Clinical Sleep Medicine*, 5(03):240–245, 2009.
- [56] M. W. Johns. A new method for measuring daytime sleepiness: the epworth sleepiness scale. *sleep*, 14(6):540–545, 1991.
- [57] R. Juszkiewicz. *Achieving a Fully Differential Output Using Single-Ended Instrumentation Amplifiers*, 2019. <https://www.analog.com/en/analog-dialogue/raqs/raq-issue-161.html>.
- [58] W. Karlen. Adaptive wake and sleep detection for wearable systems. Technical report, EPFL, 2009.
- [59] R. N. Khushaba, S. Kodagoda, S. Lal, and G. Dissanayake. Driver drowsiness classification using fuzzy wavelet-packet-based feature-extraction algorithm. *IEEE Transactions on Biomedical Engineering*, 58(1):121–131, Jan 2011.
- [60] P. Kidmose, D. Looney, and D. P. Mandic. Auditory evoked responses from ear-eeg recordings. In *Engineering in Medicine and Biology Society (EMBC), 2012 Annual International Conference of the IEEE*, pages 586–589. IEEE, 2012.

- [61] S. Labs. *Improving ADC Resolution by Oversampling and Averaging*, 2013. <https://www.silabs.com/documents/public/application-notes/an118.pdf>.
- [62] L. lan Chen, Y. Zhao, J. Zhang, and J. zhong Zou. Automatic detection of alertness/drowsiness from physiological signals using wavelet-based nonlinear features and machine learning. *Expert Systems with Applications*, 42(21):7344 – 7355, 2015.
- [63] D. S. Lauderdale, K. L. Knutson, L. L. Yan, K. Liu, and P. J. Rathouz. Sleep duration: how well do self-reports reflect objective measures? the cardia sleep study. *Epidemiology (Cambridge, Mass.)*, 19(6):838, 2008.
- [64] B.-L. Lee, B.-G. Lee, and W.-Y. Chung. Standalone wearable driver drowsiness detection system in a smartwatch. *IEEE Sensors journal*, 16(13):5444–5451, 2016.
- [65] S.-I. Lee, H. Lee, P. Abbeel, and A. Y. Ng. Efficient l1 regularized logistic regression. In *AAAI*, 2006.
- [66] J. Lewis. Fast template matching. 1995. URL http://www.scribblethink.org/Work/nvisionInterface/vi95_lewis.pdf. Cited on, page 6.
- [67] C.-T. Lin, C.-J. Chang, B.-S. Lin, S.-H. Hung, C.-F. Chao, and I.-J. Wang. A real-time wireless brain-computer interface system for drowsiness detection. *IEEE transactions on biomedical circuits and systems*, 4(4):214–222, 2010.
- [68] R. G. Lyons. *Understanding digital signal processing, 3/E*. Pearson Education India, 2004.
- [69] J.-X. Ma, L.-C. Shi, and B.-L. Lu. An eog-based vigilance estimation method applied for driver fatigue detection. *Neuroscience and Biomedical Engineering*, 2(1):41–51, 2014.
- [70] P. Matsangas and N. Shattuck. 0172 prevalence of insomnia and excessive daytime sleepiness in us navy sailors. *Journal of Sleep and Sleep Disorders Research*, 40(suppl_1):A64–A64, 2017.
- [71] Mazda. Driver attention alert. https://www.mazda.com/en/innovation/technology/safety/active_safety/daa/. [Online; accessed Apr 21, 2020].
- [72] K. B. Mikkelsen, S. L. Kappel, D. P. Mandic, and P. Kidmose. Eeg recorded from the ear: Characterizing the ear-eeg method. *Frontiers in neuroscience*, 9:438, 2015.
- [73] V. G. Motti and K. Caine. Users' privacy concerns about wearables. In *International Conference on Financial Cryptography and Data Security*, pages 231–244. Springer, 2015.
- [74] T. Nakamura, Y. D. Alqurashi, M. J. Morrell, and D. P. Mandic. Automatic detection of drowsiness using in-ear eeg. In *2018 International Joint Conference on Neural Networks (IJCNN)*, pages 1–6. IEEE, 2018.
- [75] R. Nandakumar, S. Gollakota, and N. Watson. Contactless sleep apnea detection on smartphones. In *Proceedings of the 13th annual international conference on mobile systems, applications, and services*, pages 45–57. ACM, 2015.
- [76] N. Network. *Narcolepsy Fast Facts*, 2013. <https://narcolepsynetwork.org/about-narcolepsy/narcolepsy-fast-facts/>.
- [77] A. Nguyen, R. Alqurashi, Z. Raghebi, F. Banaei-Kashani, A. C. Halbower, and T. Vu. A lightweight and inexpensive in-ear sensing system for automatic whole-night sleep stage monitoring. In *Proceedings of the 14th ACM Conference on Embedded Network Sensor Systems CD-ROM*, pages 230–244. ACM, 2016.
- [78] P. Nguyen, N. Bui, A. Nguyen, H. Truong, A. Suresh, M. Whitlock, D. Pham, T. Dinh, and T. Vu. Tyth-typing on your teeth: Tongue-teeth localization for human-computer interface. In *Proceedings of the 16th Annual International Conference on Mobile Systems, Applications, and Services*, pages 269–282. ACM, 2018.
- [79] A. D. Nordin, W. D. Hairston, and D. P. Ferris. Dual-electrode motion artifact cancellation for mobile electroencephalography. *Journal of neural engineering*, 15(5):056024, 2018.
- [80] U. D. of Health and H. Services. *Types of Sleep Studies*. <https://tinyurl.com/y232zaac>.
- [81] A. A. of Sleep Medicine. *Economic burden of undiagnosed sleep apnea in U.S. is nearly \$150B per year*. <https://tinyurl.com/yxkfe5zh>.
- [82] D. of Sleep Medicine at Harvard Medical School. *Narcolepsy Medications*, 2018. <http://healthysleep.med.harvard.edu/narcolepsy/treating-narcolepsy/medications>.
- [83] K. Onikura and K. Iramina. Evaluation of a head movement artifact removal method for eeg considering real-time processing. In *2015 8th Biomedical Engineering International Conference (BMEiCON)*, pages 1–4. IEEE, 2015.
- [84] S. Özşen, S. Güneş, and Ş. Yosunkaya. Examining the effect of time and frequency domain features of eeg, eog, and chin emg signals on sleep staging. In *2010 15th National Biomedical Engineering Meeting*, pages 1–4, April 2010.
- [85] J. Pagel. *Excessive Daytime Sleepiness*, May 2009. <https://www.aafp.org/afp/2009/0301/p391.html>.
- [86] A. Paul, L. N. Boyle, J. Tippin, and M. Rizzo. Variability of driving performance during microsleeps. 2005.
- [87] M. T. Peiris, R. D. Jones, P. R. Davidson, G. J. Carroll, and P. J. Bones. Frequent lapses of responsiveness during an extended visuomotor tracking task in non-sleep-deprived subjects. *Journal of sleep research*, 15(3):291–300, 2006.
- [88] R. W. Picard, S. Fedor, and Y. Ayzenberg. Multiple arousal theory and daily-life electrodermal activity asymmetry. *Emotion Review*, 8(1):62–75, 2016.
- [89] N. Y. post. *The revolt against Google 'Glassholes'*. <https://tinyurl.com/v9ruu6h>.
- [90] G. R. Poudel, C. R. Innes, P. J. Bones, R. Watts, and R. D. Jones. Losing the struggle to stay awake: divergent thalamic and cortical activity during microsleeps. *Human brain mapping*, 35(1):257–269, 2014.
- [91] W. Rapson. Skin contact with gold and gold alloys. *Contact Dermatitis*, 13(2):56–65, 1985.
- [92] C. M. D. W. R. T. Roehrs, T. Daytime sleepiness and alertness. In *Principles and Practice of Sleep Medicine: Fifth Edition*. Elsevier Inc., 2010.
- [93] A. Sahayadhas, K. Sundaraj, and M. Murugappan. Detecting driver drowsiness based on sensors: a review. *Sensors*, 12(12):16937–16953, 2012.
- [94] T. Sakurai. The neural circuit of orexin (hypocretin): maintaining sleep and wakefulness. *Nature Reviews Neuroscience*, 8(3):171, 2007.
- [95] M. J. Sateia. International classification of sleep disorders. *Chest*, 146(5):1387–1394, 2014.
- [96] S. Schreyer, J. A. Büttner-Ennever, X. Tang, M. J. Mustari, and A. K. Horn. Orexin-a inputs onto visuomotor cell groups in the monkey brainstem. *Neuroscience*, 164(2):629–640, 2009.
- [97] C. Schwarz, J. Gaspar, T. Miller, and R. Yousefian. The detection of drowsiness using a driver monitoring system. *Traffic injury prevention*, 20(sup1):S157–S161, 2019.
- [98] B. Sen, M. Peker, A. Cavusoglu, and F. V. Celebi. A Comparative Study on Classification of Sleep Stage Based on EEG Signals Using Feature Selection and Classification Algorithms. *Journal of Medical Systems*, 38(3):1–21, 2014.
- [99] S. H. Sheldon, R. Ferber, and M. H. Kryger. *Principles and practice of pediatric sleep medicine*. Elsevier Health Sciences, 2005.
- [100] A. Simakov and J. Webster. Motion artifact from electrodes and cables. 2010.
- [101] S. R. Sinha, L. R. Sullivan, D. Sabau, D. S. J. Orta, K. E. Dombrowski, J. J. Halford, A. J. Hani, F. W. Drislane, and M. M. Stecker. American clinical neurophysiology society guideline 1: minimum technical requirements for performing clinical electroencephalography. *The Neurodiagnostic Journal*, 56(4):235–244, 2016.
- [102] J. Skorucak, A. Hertig-Godeschalk, D. R. Schreier, A. Malafeev, J. Mathis, and P. Achermann. Automatic detection of microsleep episodes with feature-based machine learning. *Sleep*, 2019.
- [103] C. J. Smith and G. Havenith. Body mapping of sweating patterns in male athletes in mild exercise-induced hyperthermia. *European journal of applied physiology*, 111(7):1391–1404, 2011.
- [104] P. Smith, M. Shah, and N. da Vitoria Lobo. Monitoring head/eye motion for driver alertness with one camera. In *Proceedings 15th International Conference on Pattern Recognition. ICPR-2000*, volume 4, pages 636–642. IEEE, 2000.
- [105] J. Solaz, J. Laparra-Hernández, D. Bande, N. Rodríguez, S. Veleff, J. Gerpe, and E. Medina. Drowsiness detection based on the analysis of breathing rate obtained from real-time image recognition. *Transportation research procedia*, 14:3867–3876, 2016.
- [106] P. K. Sullivan, M. J. Brucker, and J. Patel. A morphometric study of the external ear: Age and sex related differences. 2010.
- [107] B. Y. Sunwoo, N. Jackson, G. Maislin, I. Gurubhagavatlula, C. F. George, and A. I. Pack. Reliability of a single objective measure in assessing sleepiness. *Sleep*, 35(1):149–158, 2012.
- [108] E.-R. Symeonidou, A. Nordin, W. Hairston, and D. Ferris. Effects of cable sway, electrode surface area, and electrode mass on electroencephalography signal quality during motion. *Sensors*, 18(4):1073, 2018.
- [109] K. Takahashi, J.-S. Lin, and K. Sakai. Neuronal activity of orexin and non-orexin waking-active neurons during wake-sleep states in the mouse. *Neuroscience*, 153(3):860–870, 2008.
- [110] R. Tan, V. Osman, and G. Tan. Ear size as a predictor of chronological age. *Archives of gerontology and geriatrics*, 25(2):187–191, 1997.
- [111] M. J. Thorpy and G. Hiller. The medical and economic burden of narcolepsy: implications for managed care. *American health & drug benefits*, 10(5):233, 2017.
- [112] S. A. Tretter. *Communication system design using DSP algorithms: with laboratory experiments for the TMS320C6713TM DSK*. Springer Science & Business Media, 2008.
- [113] K. Uehli, A. J. Mehta, D. Miedinger, K. Hug, C. Schindler, E. Holsboer-Trachslar, J. D. Leuppi, and N. Künzli. Sleep problems and work injuries: a systematic review and meta-analysis. *Sleep medicine reviews*, 18(1):61–73, 2014.
- [114] J. A. Urigüen and B. Garcia-Zapirain. EEG artifact removal – state-of-the-art and guidelines. *Journal of neural engineering*, 12(3):031001, 2015.
- [115] M. Vidal, A. Bulling, and H. Gellersen. Analysing eog signal features for the discrimination of eye movements with wearable devices. In *Proceedings of the 1st international workshop on pervasive eye tracking & mobile eye-based interaction*, pages 15–20. ACM, 2011.
- [116] Vigo. Vigo smart headset. <https://www.wearvigo.com/>. [Online; accessed Mar 28, 2019].
- [117] E. Vural, M. Cetin, A. Ercil, G. Littlewort, M. Bartlett, and J. Movellan. Drowsy driver detection through facial movement analysis. In *International Workshop on Human-Computer Interaction*, pages 6–18. Springer, 2007.
- [118] Weaver and Company. Ten20 conductive paste. <https://www.weaverandcompany.com/products/ten20/>. [Online; accessed Apr 21, 2020].

- [119] J. Webster. Interference and motion artifact in biopotentials. In *IEEE 1977 Region Six Conference Record, 1977.*, pages 53–64. IEEE, 1977.
- [120] W. Wen, D. Tomoi, H. Yamakawa, S. Hamasaki, K. Takakusaki, Q. An, Y. Tamura, A. Yamashita, and H. Asama. Continuous estimation of stress using physiological signals during a car race. *Psychology*, 8(07):978, 2017.
- [121] WIRED. *I, Glasshole: My Year With Google Glass*. <https://www.wired.com/2013/12/glasshole/>.
- [122] J. Xu, S. Mitra, C. Van Hoof, R. F. Yazicioglu, and K. A. Makinwa. Active electrodes for wearable eeg acquisition: Review and electronics design methodology. *IEEE reviews in biomedical engineering*, 10:187–198, 2017.
- [123] J. Xu, R. F. Yazicioglu, B. Grundlehner, P. Harpe, K. A. Makinwa, and C. Van Hoof. A 160 μ W 8-Channel Active Electrode System for EEG Monitoring. *IEEE Transactions on Biomedical Circuits and Systems*, 5(6):555–567, 2011.
- [124] R. Zangróniz, A. Martínez-Rodrigo, J. Pastor, M. López, and A. Fernández-Caballero. Electrodermal activity sensor for classification of calm/distress condition. *Sensors*, 17(10):2324, 2017.
- [125] Z. Zhang and J. Zhang. A new real-time eye tracking based on nonlinear unscented kalman filter for monitoring driver fatigue. *Journal of Control Theory and Applications*, 8(2):181–188, 2010.